Since January 2020 Elsevier has created a COVID-19 resource centre with free information in English and Mandarin on the novel coronavirus COVID-19. The COVID-19 resource centre is hosted on Elsevier Connect, the company's public news and information website.

Virology 388 (2009) 147–159

Contents lists available at ScienceDirect

Virology

journal homepage: www.elsevier.com/locate/yviro

Cymbidium mosaic potexvirus isolate-dependent host movement systems reveal two movement control determinants and the coat protein is the dominant

Hsiang-Chia Lu [a,1], Cheng-En Chen [a,1], Meng-Hsiun Tsai [b], Hsiang-iu Wang [c], Hong-Ji Su [a], Hsin-Hung Yeh [a,*]

[a] Department of Plant Pathology and Microbiology, National Taiwan University, 1, sec 4, Roosevelt Road, Taipei 106, Taiwan
[b] Department of Management Information Systems, National Chung Hsing University, 250, Kuo Kuang Rd., Taichung 402, Taiwan
[c] Department of Computer Science, National Tsing Hua University, 101, Section 2, Kuang-Fu Road, Hsinchu 30013, Taiwan

ARTICLE INFO

Article history:
Received 19 December 2008
Returned to author for revision
28 January 2009
Accepted 28 February 2009
Available online 5 April 2009

Keywords:
Cymbidium mosaic virus
Potexvirus
Host range
Virus movement

ABSTRACT

Little is known about how plant viruses of a single species exhibit different movement behavior in different host species. Two *Cymbidium mosaic potexvirus* (CymMV) isolates, M1 and M2, were studied. Both can infect *Phalaenopsis* orchids, but only M1 can systemically infect *Nicotiana benthamiana* plants. Protoplast inoculation and whole-mount *in situ* hybridization revealed that both isolates can replicate in *N. benthamiana*; however, M2 was restricted to the initially infected cells. Genome shuffling between M1 and M2 revealed that two control modes are involved in CymMV host dependent movement. The M1 coat protein (CP) plays a dominant role in controlling CymMV movement between cells, because all chimeric CymMV viruses containing the M1 CP systemically infected *N. benthamiana* plants. Without the M1 CP, one chimeric virus containing the combination of the M1 triple gene block proteins (TGBps), the M2 5′ RNA (1–4333), and the M2 CP effectively moved in *N. benthamiana* plants. Further complementation analysis revealed that M1 TGBp1 and TGBp3 are co-required to complement the movement of the chimeric viruses in *N. benthamiana*. The amino acids within the CP, TGBp1 and TGBp3 which are required or important for CymMV M2 movement in *N. benthamiana* plants were mapped. The required amino acids within the CP map to the predicted RNA binding domain. RNA–protein binding assays revealed that M1 CP has higher RNA binding affinity than does M2 CP. Yeast two-hybrid assays to detect all possible interactions of M1 TGBps and CP, and only TGBp1 and CP self-interactions were observed.

Introduction

Viruses have a defined, restricted host range, which varies among different viruses, or sometimes even different isolates of the same virus species. For example, *Cucumber mosaic virus* (CMV) has a host range of more than 1000 plant species in 85 families, including monocotyledonous and dicotyledonous plants, and by contrast, *Barley stripe mosaic virus* (BSMV) has a confined natural host to barley (ICTVdB: The Universal Virus Database of the International Committee on Taxonomy of Viruses [http://www.ictvdb.iacr.ac.uk/Ictv/fr-index.htm.]; (Timian, 1974). Disease may occur when a particular virus adapts and/or shifts to a new host, for which there are many examples in plants and even humans (e.g., severe acute respiratory syndrome).

Successful infection of a plant host requires that plant viruses achieve (i) replication in the initially infected cells, (ii) movement through plasmodesmata to adjacent cells from the initial infected site and (iii) long-distance spread in a host through the vascular tissue. Plant viruses possess only limited genetic information; hence, to complete their infection cycles, interactions between virus proteins and necessary host factors is critical. For a virus to successfully infect different plant hosts, the limited number of virus-encoded proteins must have the ability to recognize and interact with factors in different hosts for a successful infection. For some plant viruses, host plants restrict viral cell-to-cell movement rather than viral replication, which results in a subliminal infection (Cheo, 1970; Sulzinski and Zaitlin, 1982). In other cases, viruses may move from cell-to-cell, but the plant prevents viral long-distance spread (Fujita et al., 1996; Saenz et al., 2002; Wang et al., 1998). Failure to accomplish any of the stages can be thought of as resistance.

In our previous studies, we collected several isolates of *Cymbidium mosaic virus* (CymMV) for construction of virus-induced gene silencing vectors for orchid functional genomic studies (Lu et al., 2007). CymMV is a prevalent orchid virus and belongs to the genus *Potexvirus* in the family *Flexiviridae* (Adams et al., 2005b). The recorded natural host range is largely limited to species belonging to *Orchidaceae* (ICTVdB: The Universal Virus Database of the International Committee on Taxonomy of Viruses [http://www.ictvdb.iacr.ac.uk/Ictv/fr-index.htm.];(Adams et al., 2005a; Zettler et al., 1990). Interestingly, we found two distinct CymMV isolates, M1 and M2, both of which can infect *Phalaenopsis* orchids, but only M1 can systemically infect *Nicotiana benthamiana* plants. Because both isolates can systemically infect orchids, this suggests that viral-encoded

* Corresponding author. Fax: +886 2 23636490.
E-mail address: hyeh@ntu.edu.tw (H.-H. Yeh).
[1] Both authors contributed equally.

0042-6822/$ – see front matter © 2009 Elsevier Inc. All rights reserved.
doi:10.1016/j.virol.2009.02.049

replication and movement proteins are functional in orchids. However, because only M1 can systemically infect *N. benthamiana* plants this suggests that M1-encoded proteins could interact successfully with factors in both plant species to allow a systemic infection, but M2-encoded proteins do not. M1 and M2 share very high nucleotide sequence identity (97%), which suggests that subtle differences contribute to the differences in host reaction.

Viruses in the genus *Potexvirus* have monopartite, positive-sense single-strand RNA genomes (Adams et al., 2005a). Studies of potexviruses have contributed importantly to our understanding of the complexity of the mechanisms of plant virus movement within plants (Lucas, 2006; Verchot-Lubicz, 2005; Verchot-Lubicz et al., 2007). Comprehensive studies of potexviruses has revealed that triple gene block proteins (TGBps) and coat proteins (CP) work cooperatively to promote viral movement between cells and long-distance in their plant hosts (Bayne et al., 2005; Beck et al., 1991; Chapman et al., 1992; Fedorkin et al., 2001; Forster et al., 1992; Ju et al., 2007; Krishnamurthy et al., 2003; Lin et al., 2006; Lough et al., 1998, 2000; Mitra et al., 2003; Tamai and Meshi, 2001; Verchot-Lubicz, 2005). The current model suggests that TGBp1 increases the plasmodesmatal size-exclusion limit and moves into neighboring cells to suppress RNA silencing (Bayne et al., 2005; Howard et al., 2004); both TGBp1 and CP bind viral RNA (vRNA) forming viral ribonucleoprotein complexes (vRNP; (Karpova et al., 2006; Lough et al., 2000, 2001); the complex is then delivered by TGBp2 induced vesicles (containing TGBp3) to plasmodesmata, and through plasmodesmata to neighboring cells; later, after the free form of TGBp1 binds membrane-associated TGBp2 and/or TGBp3, then TGBp1 (on the vRNP complex) binds with the membrane-associated TGBp1 complex (TGBp1 with TGBp2 or TGBp3) to form a membrane-bound complex and begin new rounds of replication (Verchot-Lubicz, 2005).

Interactions between TGBp1 and CP (Karpova et al., 2006; Lough et al. 2000), and TGBp1 self-interactions (Samuels et al., 2007) have been reported, and those between TGBp1 and TGBp2, and between TGBp1 and TGBp3 have been suggested (Karpova et al., 2006; Krishnamurthy et al., 2002; Lough et al., 2000; Verchot-Lubicz, 2005; Yang et al., 2000). Interestingly, *trans*-complementation of TGBps between potexvirus species was not successful, and it was suggested that species-specific interactions among potexvirus movement proteins are obligatory for cell-to-cell movement (Lin et al., 2006). However, *trans*-complementation of movement defective potexviruses by movement proteins derived from *Tomato mosaic tobamovirus*, *Crucifer tobamovirus* and *Red clover necrotic mosaic dianthovirus* have been reported (Morozov et al., 1997).

Although the movement of plant viruses, including potexviruses, has been extensively studied, little is known about how plant viruses of a single species exhibit different movement behavior in different host species. In this study, we aimed to use our CymMV-M1, -M2 and *N. benthamiana* system to study the molecular basis of CymMV isolate-dependent host movement determinants, and to resolve the mechanism involved in CymMV translocation. Our studies not only help to identify the molecular determinants of CymMV isolate-dependent host movement, but other phenomena that are not easily resolved by studies using a single isolate. Finally, our efforts revealed two control behaviors, dominant and matching modes, involved in CymMV host dependent movement, and showed that the binding strength between the CymMV CP and genomic RNA is correlated with the dominant control mode.

Results

Construction of CymMV infectious clones and derived expression vectors

The construction of the infectious clone of the isolates M1 (pCymMV-M1, Fig. 1) and its derived expression vector (pCymMV-M1-GFP, Fig. 1) engineered with the green fluorescent protein (GFP) was previously described (Lu et al., 2007). We followed the same strategy to construct the M2 infectious clone (pCymMV-M2, Fig. 1) and its derived expression vector (pCymMV-M2-GFP, Fig. 1). *Phalaenopsis amabilis* var. *formosa* and *Nicotiana benthamiana* plants were inoculated with transcripts from pCymMV-M1 and pCymMV-M2, and nucleic acids were extracted from the inoculated and upper, non-inoculated leaves of pCymMV-M1 and pCymMV-M2-inoculated plants 14 days post-inoculation. Similar to our previous findings, both pCymMV-M1 and pCymMV-M2 systemically infected *Phalaenopsis* orchids (Fig. 1B), but only pCymMV-M1 systemically infected *N. benthamiana* (Fig. 1C).

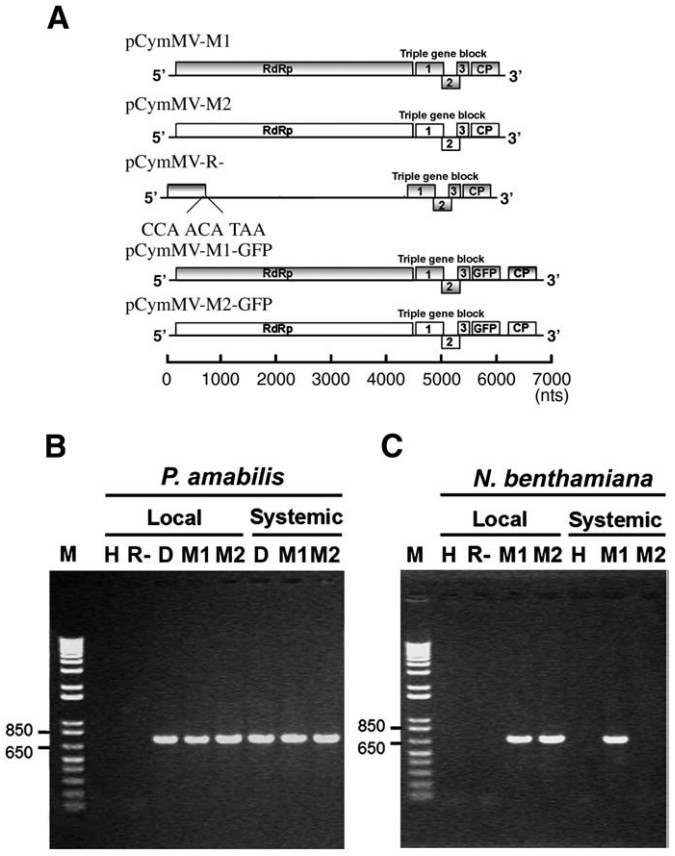

Fig. 1. Schematic representation of CymMV cDNA infectious clones (A) and detection of CymMV in infected *Phalaenopsis amabilis* (B) and *Nicotiana benthamiana* (C) by RT-PCR. (A) Rectangles represent open reading frames encoded by CymMV genomic RNA. RNA-dependent RNA polymerase (RdRp), triple gene block ORFs 1, 2, and 3, capsid protein (CP) and green fluorescent protein (GFP). The mutated sequences in pCymMV-R- are indicated by bold letters. Scale bar, in nucleotides, is shown at the bottom. *P. amabilis* var. *formosa* (B) and *N. benthamiana* (C) inoculated with buffer (H), pCymMV-R- transcripts (R-), pCymMV-M1 transcripts (M1) and pCymMV-M2 transcripts (M2), with CymMV-infected *Phalaenopsis* used as a positive control (D). Total nucleic acids were extracted from CymMV-inoculated and upper leaves distal from the inoculation point, and CymMV was detected by RT-PCR. pCymMV-R- is a replication-incompetent clone used as a negative control (see Materials and Methods). Numbers at the left correspond to positions of marker DNAs (M) (sizes in 1000 base pairs).

Replication of CymMV isolates in N. benthamiana protoplasts

To test whether CymMV-M2 can replicate in *N. benthamiana*, protoplasts were inoculated with transcripts from pCymMV-M1, pCymMV-M2, pCymMV-M1-GFP and pCymMV-M2-GFP. Illumination of GFP was observed from pCymMV-M1-GFP and pCymMV-M2-GFP

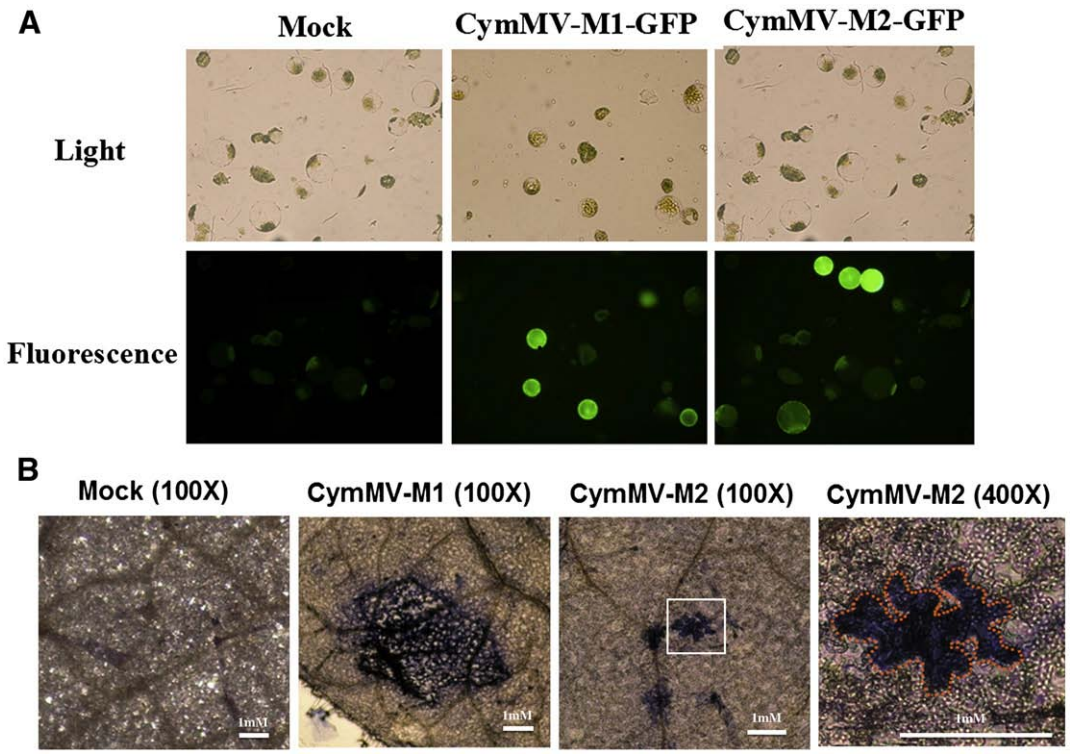

Fig. 2. Protoplast inoculation assay and whole-mount *in situ* hybridization. (A) A total of 5×10^5 *N. benthamiana* protoplasts were inoculated with water (Mock) and transcripts of pCymMV-M1-GFP and pCymMV-M2-GFP. Cells were examined 14 h post-inoculation by light and fluorescent microscopy. (B) Leaves were first fixed with 1× phosphate buffered saline solution (pH 7.2) containing 0.1% Tween 20, 0.08 M EGTA, 10% DMSO and 5% paraformaldehyde then hybridized with a Dig-labeled CymMV CP probe. The mock, CymMV-M1 and CymMV-M2 infected leaves are indicated. The white rectangle indicates the region selected for further zooming. Magnification and scale bars in micrometers (μm) are indicated. The red "jigsaw shaped" pattern indicates a single epidermal cell.

infected protoplasts at 14 h post-inoculation (Fig. 2). Northern blot hybridization also indicated that pCymMV-M1 and pCymMV-M2 replicated in *N. benthamiana* protoplasts (Fig. 3I).

Subliminal infection of CymMV-M2 in N. benthamiana

To next analyze why M2 failed to accomplish systemic infection in *N. benthamiana* plants, more plants were inoculated with transcripts from pCymMV-M1-GFP and pCymMV-M2-GFP. Because of limited expression of GFP of both pCymMV-M1-GFP and pCymMV-M2-GFP in plants of *N. benthamiana*, we therefore inoculated *N. benthamiana* with transcripts of pCymMV-M1 and pCymMV-M2 and assayed by whole-mount *in situ* hybridization 14 days post-inoculation. pCymMV-M1 moved from the inoculation foci and infected a broader area of leaves (Fig. 2B), whereas pCymMV-M2 was limited to the initial inoculated cells and did not spread from cell to cell, thus resulting only in subliminal infections (Fig. 2B).

Genome shuffling between CymMV-M1 and -M2 for complementation analysis

PVX TGBps 1–3 and CP proteins are known to be required for virus cell-to-cell movement (Bayne et al., 2005; Chapman et al., 1992; Krishnamurthy et al., 2002, 2003; Lough et al., 2000; Morozov and Solovyev, 2003; Tamai and Meshi, 2001; Verchot-Lubicz, 2005). To determine if specific M1 gene(s) can complement M2 for virus movement, we constructed a series of M1 and M2 chimeric viruses (Fig. 3). *N. benthamiana* protoplasts and plants were inoculated with transcripts derived from each construct. Northern blot hybridization revealed that each virus replicated in *N. benthamiana* protoplasts (Fig. 3I), and statistics analysis (ANOVA) of real-time RT-PCR quantification of average relative percentage (from 3 independent experiments) of CymMV RNA from CymMV clone-infected protoplasts at 24 h post-inoculation revealed no significant difference in percentage between these clones ($P=0.88$).

Systemic infections were monitored by performing RT-PCR on leaves distal from the inoculation site at 2 weeks post-inoculation (Figs. 3A–H). These analyses showed that if the CymMV construct contained the M1 CP, the virus systemically infected *N. benthamiana* plants (Figs. 3A, C, E, H). One notable exception was the pCymMV-M2/TGB-M1. This construct contained the M2 CP and 5′ RNA sequence (1–4333; include the whole RNA-dependent RNA polymerase encoding region), but also the M1 triple gene block ORFs (Fig. 3F).

To identify whether TGBps 1–3 were all necessary to complement the systemic infection of pCymMV-M2/TGB-M1, we performed genome shuffling between M1 and M2 TGBps 1–3, and constructed chimeric viruses (Figs. 4A–H). *N. benthamiana* protoplasts and plants were inoculated with transcripts derived from each construct. All constructs were replication competent in protoplasts as assayed by northern blot hybridization (Fig. 4I), and statistics analysis (ANOVA) of real-time RT-PCR quantification of average relative percentage (from 3 independent experiments) of CymMV RNA from CymMV clone-infected protoplasts at 24 h post-inoculation revealed no significant difference in percentage between these clones ($P=0.91$).

Systemic infection, as detected by RT-PCR at 2 weeks post-inoculation (Figs. 4A–H), indicated that only chimeric viruses containing the M1 TGBp1 and TGBp3 moved systemically (Fig. 4G).

Because these results were complicated, we used the Karnaugh Maps (Harrison, 1969) tabular logical calculation to explore possible explanations (data not shown). The results of these analyses are summarized in Fig. 5. The analysis revealed that two control modes, which we termed dominant and matching control modes, are involved in CymMV movement. The M1 CP plays a dominant role in controlling the trafficking of the infection agents within plants. Without the M1 CP, another control mode, which required correct

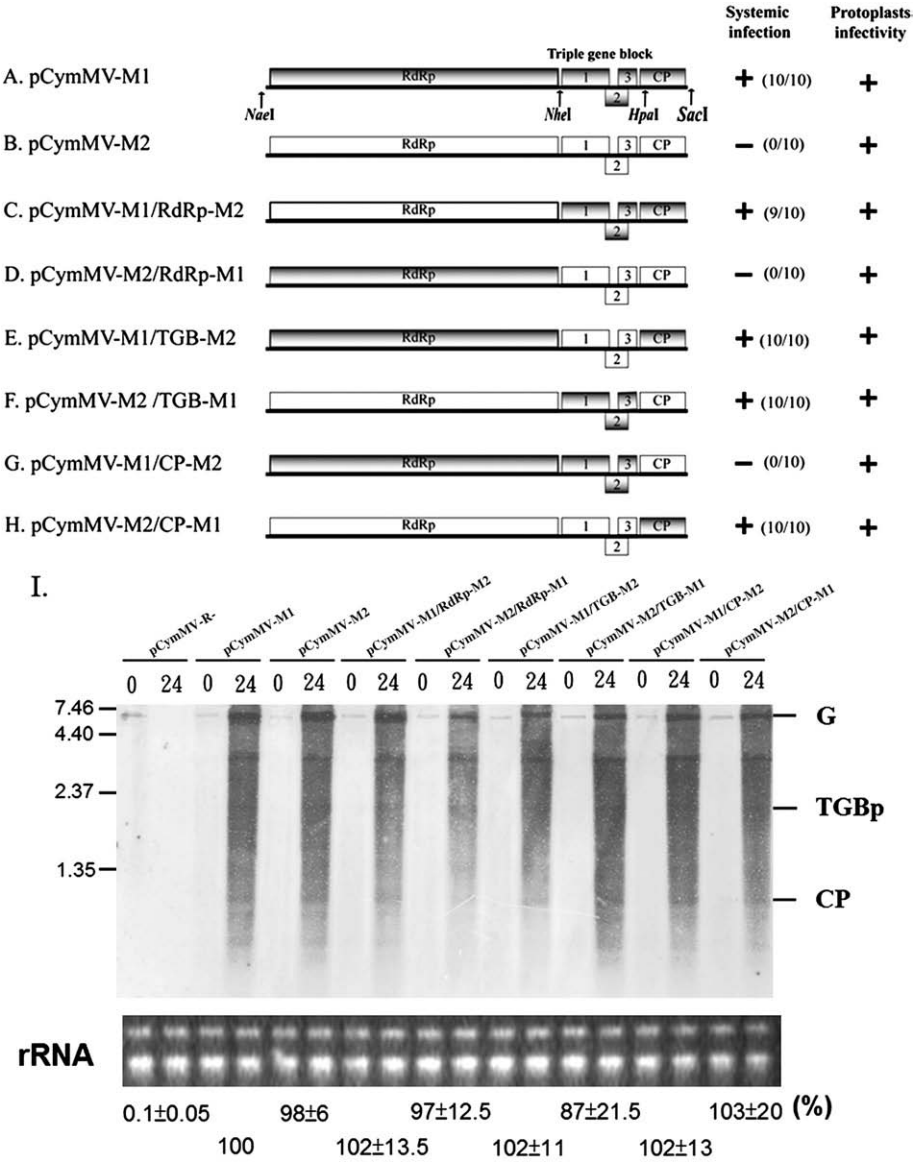

Fig. 3. Schematic representation of genome organization and infectivity assay of the parental CymMV-M1 and CymMV-M2 and the derived chimeric constructs. (A–H). Rectangles represent open reading frames encoded by CymMV genomic RNA, RNA-dependent RNA polymerase (RdRp), triple gene block (TGB) ORFs 1, 2, and 3 and capsid protein (CP). Sequences corresponding to pCymMV-M1 and pCymMV-M2 are indicated by gray and white rectangles, respectively. The restriction enzyme sites for constructing chimeric viruses are indicated. (Although HpaI sites are located 129 nt downstream of CP translation start sites, the amino acid sequences in the regions between M1 and M2 are identical.) Clones competent in protoplast accumulation and systemic infection in *N. benthamiana* are indicated by +, and the ratio of systemic infected to total inoculated plants is indicated. Systemic infection was detected 2 weeks post-inoculation by RT-PCR. (I) Protoplast infectivity was detected 24 h post-inoculation by northern blot hybridization, and the ribosomal RNA used for a loading control are indicated. Genomic RNA (G), TGBp, and CP subgenomic RNA are indicated. The pCymMV-R- used as a negative control is illustrated in Fig. 1. The average percentage of relative real-time RT-PCR quantification (from 3 independent experiments) of CymMV RNA from CymMV clone-infected protoplasts at 24 h post-inoculation is indicated. The accumulation of pCymMV-M1 was set at 100% for relative quantification. Numbers at the left correspond to positions of marker RNAs (sizes in 1000 nucleotides) analyzed in the same gel.

matching of the particular movement accessory components including the M2 5′ RNA (1–4333), M1 TGB p1, M1TGBp3, and M2 CP was also identified.

Mapping the amino acids on CymMV CP that are important for systemic infection of N. benthamiana plants

Our studies indicated that the M1 CP plays a major role in determining CymMV movement in *N. benthamiana*. Because M1 and M2 share a very high nucleotide sequence identity (97%), we attempted to identify the individual, important amino acids of the CP that allowed for the CymMV systemic infection of *N. benthamiana* plants. Sequence alignment of the M1 and M2 CPs revealed only four amino acid differences (Figs. 6A, B). Site-directed mutagenesis was then performed to construct a series of CymMV-M2 CP mutants containing specific M1 CP amino acids (Figs. 6C–I). All constructs were replication competent in protoplasts as assayed by northern blot hybridization (Fig. 6J), and statistics analysis (ANOVA) of real-time RT-PCR quantification of average relative percentage (from 3 independent experiments) of CymMV RNA from CymMV clone-infected protoplasts at 24 h post-inoculation revealed no significant difference in percentage between these clones ($P = 0.83$). Transcripts derived from each construct were used to inoculate *N. benthamiana* plants. These analyses showed that the CP amino acid G82A and L89P changes were both required for M2 to systemically infect *N. benthamiana* plants (Figs. 6C, H). Interestingly, these amino acids are located within the previously predicted RNA binding domain of the CP (Fig. 7A).

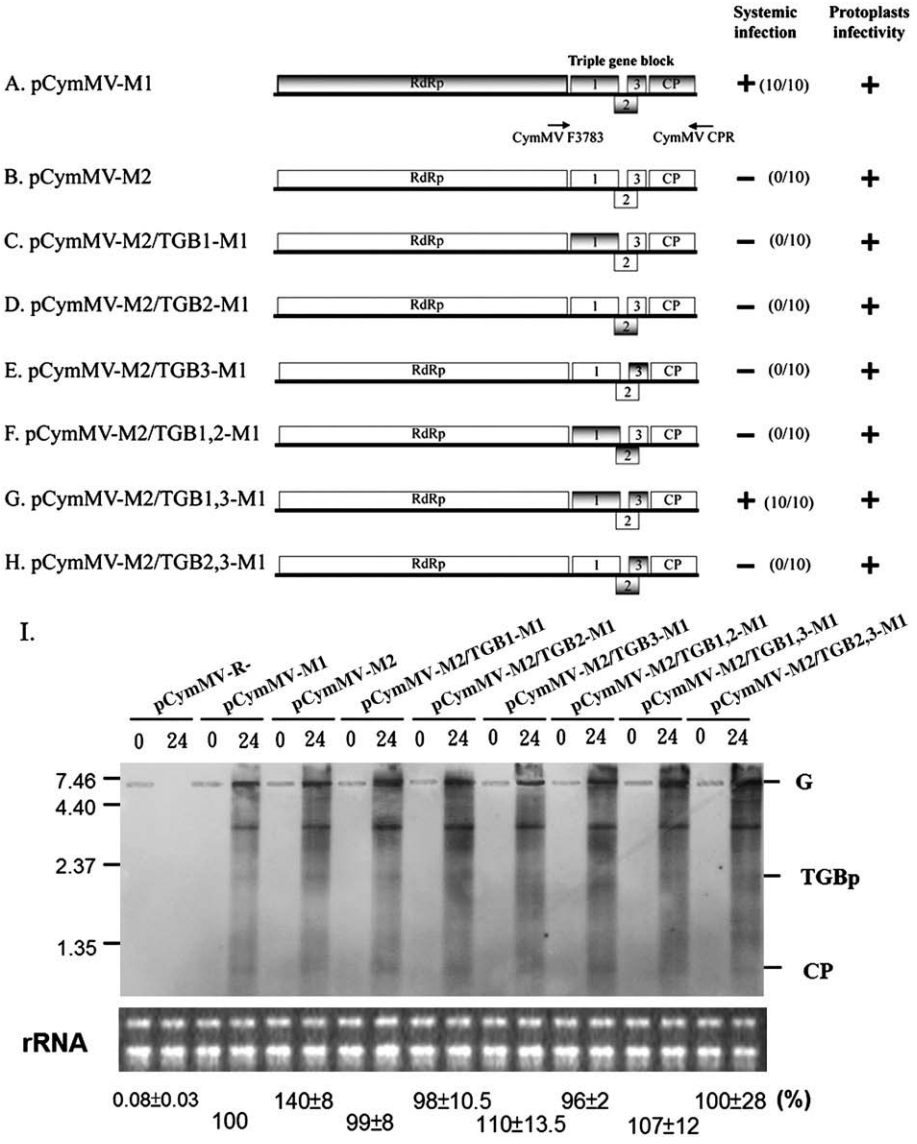

Fig. 4. Schematic representation of genome organization and infectivity assay of the parental CymMV-M1 and CymMV-M2 and the derived TGBp1 and TGBp3 chimeric constructs in *N. benthamiana*. (A–H). Sequences corresponding to pCymMV-M1 and pCymMV-M2 are indicated by gray and white rectangles, respectively. Clones competent in protoplast accumulation and systemic infection are indicated by +, and the ratio of systemic infected to total inoculated plants is indicated. Systemic infection was detected 2 weeks post-inoculation by RT-PCR. (I) Protoplast infectivity was detected 24 h post-inoculation by northern blot hybridization, and the ribosomal RNA used for a loading control are indicated. Genomic RNA (G), TGBp, and CP subgenomic RNA are indicated. The pCymMV-R- used as a negative control is illustrated in Fig. 1. The average percentage of relative real-time RT-PCR quantification (from 3 independent experiments) of CymMV RNA from CymMV clone-infected protoplasts at 24 h post-inoculation is indicated below the gels. The accumulation of pCymMV-M1 was set at 100% for relative quantification. Numbers at the left correspond to positions of marker RNAs (sizes in 1000 nucleotides) analyzed in the same gel. The primers CymMV F3783 and CymMV CPR used in construction all chimeric viruses are indicated. Other primers used in construction individual chimeric viruses are in Supplementary Table S1. Numbers at the left correspond to positions of marker RNAs (sizes in 1000 nucleotides) analyzed in the same gel.

Binding affinity assay between CymMV M1 and M2 CPs and RNAs

It has been previously reported that the CP is involved in forming ribonucleoprotein complexes and is an important step for potexvirus movement (Karpova et al., 2006; Lough et al., 2000, 2001). Our results indicated that the important amino acids of the CP that allowed for the CymMV systemic infection are located within the previously predicted RNA binding domain (Fig. 7A; 1). Thus, it might be that the binding affinity between CPs and RNAs of CymMV M1 and M2 may play roles in CymMV movement, and therefore we attempted to analyze and compare their binding affinities. Because the whole genomic RNA of CymMV is 6227 nucleotides in length, which made conventional gel-shift assays difficult, we performed modified RNA–protein pull-down assays for our analyses. Our data indicated that CymMV M1 CP has a higher binding affinity as compared to CymMV M2 CP (Fig. 7D, lanes 1–4). We then also performed CP and CymMV RNA binding assays on CymMV M2 CP with the amino acid changes G82A and L89P (derived from clone pCymMV-M2-CP-GL/AP; Fig. 6H). The results indicated that with these amino acid changes (G82A and L89P), the binding affinity was higher as compared to wild-type CymMV-M2 CP (Fig 7D, lanes 3,4,5 and 6).

Interaction analysis of TGBps by use of yeast two-hybrid assay

Our analysis also indicated that both M1 TGBp1 and TGBp3 were co-required for CymMV M2 chimeric viruses to move systemically in *N. benthamiana* plants (Fig. 4G), and was consistent with previous suggestions indicating interactions between potexvirus TGBp1 and TGBp3 (Lucas, 2006; Verchot-Lubicz, 2005; Verchot-Lubicz et al., 2007). Therefore, we attempted to determine if specific interactions occurred within and between CymMV TGBps and CP by use of the

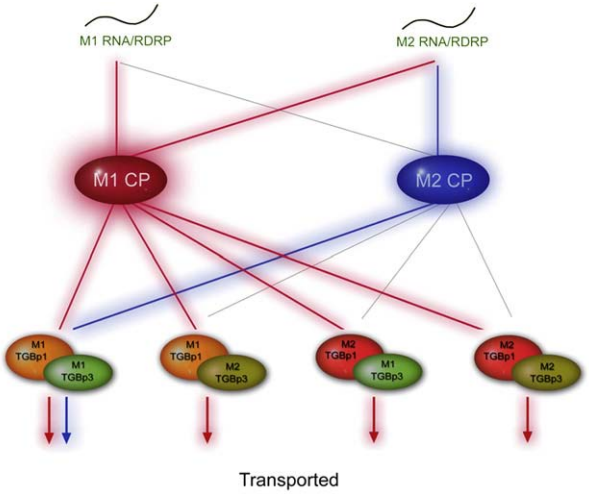

Fig. 5. Model of dominant and matching control modes in *Cymbidium mosaic* potexvirus movement between cells. The M1 CP plays a dominant role in controlling the trafficking of the infection between cells. However, besides the CP-mediated dominant control, another control mode that requires correct matching of TGBp1, TGBp3, CP and 5' RNA also allowed the movement of CymMV between cells. The red and blue lines indicate the functional combination of movement accessory components in dominant and matching control modes, respectively. The gray lines indicated the incorrect matching of movement accessory components. The M1 and M2 RNAs, TGBp1s, TGBp2s, TGBp3s and RNA-dependent RNA polymerase (RdRp) are indicated.

yeast two-hybrid assay. The results were similar to those previously reported in PVX TGBps and CP (Samuels et al., 2007); where only self interaction of TGBp1 and CP were identified (Table 1).

Mapping the amino acids on TGBp1 and TGBp3 of CymMV that are important for systemic infection of N. benthamiana

Sequence alignment analysis revealed 4 and 2 amino acid differences within the TGBp1 and TGBp3 between CymMV-M1 and CymMV-M2, respectively (Figs. 8A, B). Loss-of-function assays were performed by using site-directed mutagenesis to substitute TGBp1 and TGBp3 with the 4 and 2 amino acids derived from M2 TGBp1 and TGBp3, respectively (Figs. 8C–H). *N. benthamiana* plants were inoculated with transcripts derived from each construct, and systemic infection was analyzed by RT-PCR (Fig. 8). The chimeric viruses with either amino acids Y44H and H94R changes in M1 TGBp1 failed to move systemically (Figs. 8C, D). Although the chimeric viruses with either amino acids L8Q or A71S changes in the M1 TGBp3 did move systemically, the ratio of systemically infected plants was much reduced (Figs. 8G, H).

To further characterize whether Y^{44} and/or H^{94} in TGBp1 are required for M2 to systemically infect *N. benthamiana* plants, site-directed mutagenesis was conducted on pCymMV-M2/TGB3-M1 (Fig. 4E) to construct M2 clones substituted with H44Y and R94H at TGBp1, either individually or simultaneously (Figs. 8I–K). Both Y and H at TGBp1 positions 44 and 94 were required for M2 (pCymMV-M2/TGB3-M1) to systemically infect *N. benthamiana* plants (Fig. 8K). Mutants having only one of these changes failed to move systemically (Figs. 8I, J). Similarly, site-directed mutagenesis was conducted on pCymMV-M2/TGB1-M1 (Fig. 4C) and pCymMV-M2-TGB3-M1-TGB1 HR/YH (Fig. 8K) to construct clones substituted with Q8L and/or S71A at TGBp3 (Fig. 8L–O). Both Q8L and/or S71A in M2 TGBp3 were important but not required for M2 to systemically infect *N. benthamiana*. Mutants having only one of these changes moved systemically, but the ratio of systemically infected plants was much reduced (Figs. 8G–O). The Y^{44} (position 44) and H^{94} in TGBp1 are located within the previous predicted NTP/helicase domain but not in the identified conserved motifs (Kadare and Haenni, 1997; Kalinina et al., 2002; Leshchiner et al., 2006), and L^{8} and A^{71} in TGBp3 are also not located in the previously identified *trans*membrane domain (Fig. 9B;21).

All constructs used in Fig. 8 were replication competent in protoplasts as assayed by northern blot hybridization (Fig. 8P), and statistics analysis (ANOVA) of real-time RT-PCR quantification of the average relative percentage (from 3 independent experiments) of CymMV RNA from CymMV clone-infected protoplasts at 24 h post-inoculation revealed no significant difference in percentage between these clones ($P = 0.92$).

Discussion

Our studies comparing CymMV isolate-dependent host movement provides new and important information on the molecular basis of how viruses of the same species can move in different host plants. We also demonstrate complex aspects of potexvirus movement not easily identified by studies using a single isolate. The more detailed resolution of these phenomena, as we demonstrate in this paper, will further help to dissect the mechanisms of potexvirus movement in plants.

Our data indicated that M1-encoded CP plays a major role for CymMV in systemic infection of *N. benthamiana* plants (Fig. 5). In all our CymMV clones, if the constructs contained the M1 CP, the virus systemically infected *N. benthamiana* plants (Figs. 3A, C, E, H). Interestingly, our data also showed that if CP was not properly functional (e.g., M2 CP), alterations in TGBps (e.g., M1 TGBp1 and 3) may compensate for the function of CP and allow CymMV to systemically infect *N. benthamiana* plants (Fig. 3F). In addition, when comparing pCymMV-M2/TGB-M1 and pCymMV-M1/CP-M2 (Figs. 3F and G), only pCymMV-M2/TGB-M1 was movement competent. The TGBps and CP are the same in both chimeric viruses. These data indicate that another control mode which required correct matching of the particular movement accessory components (M2 5′ RNA, TGBp1 and TGBp3 and M2 CP) also allowed the systemic infection of CymMV in *N. benthamiana* (Fig. 3F and Fig. 5). Thus, our data suggested two control modes are involved in CymMV movement in *N. benthamiana*.

The nature of the CymMV vRNP that moves between cells remain a subject for study (Verchot-Lubicz et al., 2007), and two forms, one is the linear vRNP formed by TGBp1, vRNA and CP (Lough et al., 2000) and another is virion or altered virion with a single-tailed particle comprising RNA, CP and TGBp1 (Cruz et al., 1998; Karpova et al., 2006). However, no matter what the proposed form of vRNP that moves between cells, all data suggest that potexvirus CP and vRNA are involved in forming the vRNP which traffics to the plasmodesmata. Our analysis indicated that the CymMV CP-vRNA binding affinity likely plays an important role in CymMV movement in *N. benthamiana* plants. Therefore, it is possible that the binding between CP-vRNA may affect the nature of vRNP; thus affecting the movement of CymMV in different hosts.

Our data also suggested that different combinations of CP-vRNA required different degrees of help from TGBps for movement (Figs. 3,4). When the binding between CP-vRNA is higher (Fig. 7 D), the need for TGBps in CymMV movement is more flexible (Figs. 3A, C, E, H); however, when the binding between CP-vRNA is weaker, the need for TGBps in CymMV movement is critical and only certain combinations of CymMV movement accessory components allowed for CymMV movement (Figs. 3B, F, 4G). It has been previously reported that in systemic hosts of PVX, the movement of TGBps are host dependent (Krishnamurthy et al., 2002; Yang et al., 2000). Because in different hosts the cellular conditions and morphology are different, it is possible that potexviruses may use different strategies to adapt to different hosts. Adjusting movement accessory components could be an efficient way to generate the diversity of functions in response to changes of cellular conditions and provide flexibility for virus movement in different hosts, and thus could be an advantage for viruses with modular designed movement proteins (Morozov and Solovyev, 2003).

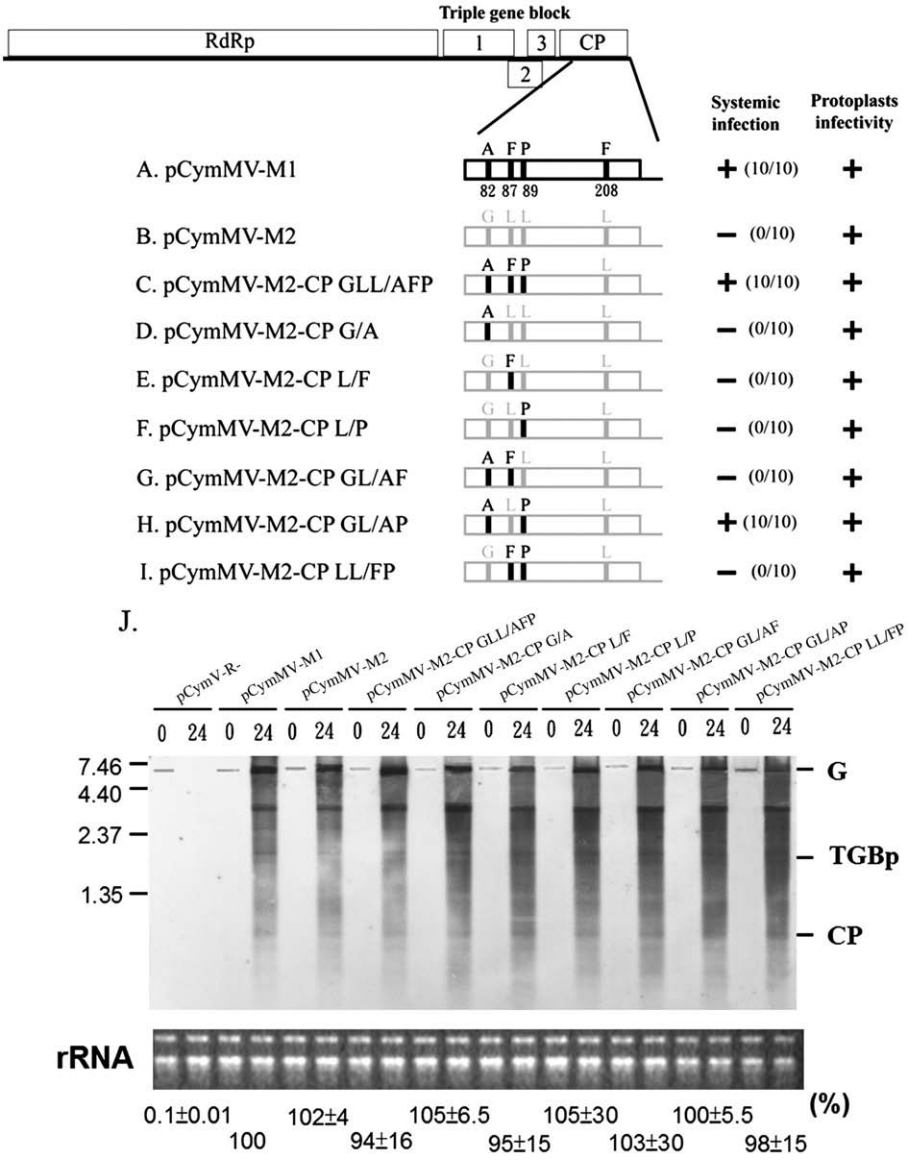

Fig. 6. Schematic representation of capsid protein (CP) mutants and infectivity assays. (A–I). Rectangles represent open reading frames encoded by CymMV genomic RNA, RNA-dependent RNA polymerase (RdRp), triple gene block ORFs 1, 2, and 3 and capsid protein (CP). Black and gray lines in the CP regions indicate the different amino acids found between pCymMV-M1 and pCymMV-M2, respectively. Position of amino acids is indicated. Chimeric viruses competent in protoplast accumulation and systemic infection in *N. benthamiana* plants are indicated by +, and the ratio of systemic infected/total inoculated plants is indicated. Systemic infection was detected 2 weeks post-inoculation by RT-PCR. (J) Protoplast infectivity was detected 24 h post-inoculation by northern blot hybridization, and the ribosomal RNA used for a loading control are indicated. Genomic RNA (G), TGBp, and CP subgenomic RNA are indicated. The pCymMV-R- used for a negative control is illustrated in Fig. 1. The pCymMV-R- used as a negative control is illustrated in Fig. 1. The average percentage of relative real-time RT-PCR quantification (from 3 independent experiments) of CymMV RNA from CymMV clone-infected protoplasts at 24 h post-inoculation is indicated below the gels. The accumulation of pCymMV-M1 was set at 100% for relative quantification. Numbers at the left correspond to positions of marker RNAs (sizes in 1000 nucleotides) analyzed in the same gel.

Although interactions between potexvirus TGBp1 and TGBp2 and between TGBp1 and TGBp3 have been suggested (Karpova et al., 2006; Krishnamurthy et al., 2002; Lough et al., 2000; Verchot-Lubicz, 2005; Yang et al., 2000), the interactions have yet to be proven. Interestingly, our data, showed that CymMV M1-encoded TGBp1 and TGBp3 are co-required for M2 systemic infection of *N. benthamiana* (Fig. 4G); which support the hypothesis for interactions between TGBp1 and TGBp3. However, the results of our yeast two-hybrid analysis were similar to those that have been recently reported showing that TGBp1 was self-associated, but showed no interactions between TGBp1 and TGBp2 or TGBp3 (Samuels et al., 2007). Thus, the interactions may not occur physically, or the interactions could be transient and not easily detected.

Within the potexvirus TGBp1, the NTPase/helicase domains have been predicated, and 7 conserved regions including two canonical motifs of NTPase, DEY and GKS, were identified (Fig. 9; Kadare, and Haenni, 1997; Kalinina et al., 2002; Leshchiner et al., 2006). Although, currently the roles of NTPase/helicase domains in potexvirus movement have not been well established (Verchot-Lubicz et al., 2007), mutations eliminating the DEY motif affects the protein subcellular targeting and mutations eliminating the DEY and GKS motifs inhibit the ability of TGBp1 to increase plasmodesmata size-exclusion limits as well as virus movement (Angell et al., 1996; Lough et al., 1998; Morozov et al., 1999). The amino acids identified in CymMV TGBp1 that are required for CymMV-M2 movement in *N. benthamiana* are within the NTPase/helicase domain, but not in the conserved motifs (Fig. 9). The amino acids are also not in the positions within the NTPase/helicase domain previously reported as essential for *Bamboo mosaic potexvirus* movement (Lin et al., 2004). Within the potexvirus TGBp3, a transmembrane domain has been previously reported. PVX

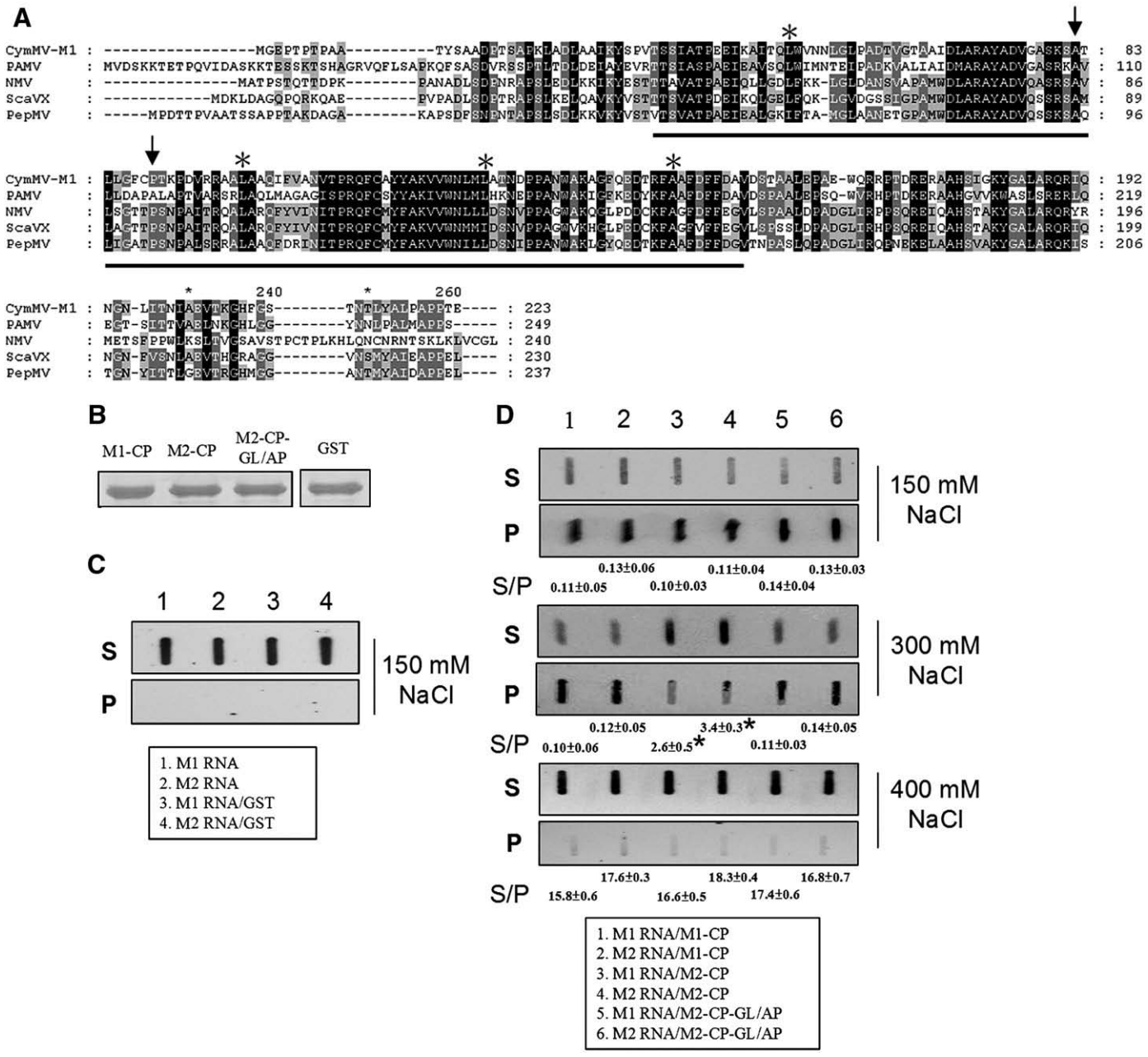

Fig. 7. The amino acid sequence alignment of predicted RNA binding domain of potexvirus CPs and slot-blot detection of biotin-labeled CymMV RNAs. (A) The amino acid sequence alignment of predicted RNA binding domain were conducted by use of clustal X 1.83 (Thompson et al., 1997). The previously identified conserved positive charged amino acids are indicated by stars (Abouhaidar and Lai, 1989). The arrows indicate the amino acids important for pCymMV-M2 to systemically infect *N. benthamiana*. The viruses, abbreviation and accession number used in alignment are described below. *Cymbidium mosaic virus* (CymMV, accession number AY571289); *Potato aucuba mosaic virus* (PAMV, accession number NC_003632; *Narcissus mosaic virus* (NMV, accession number NC_001441); *Scallion virus* X (ScaVX, accession number NC_003400); *Papaya mosaic virus* (PapMV, accession number NC_001748). (B). The concentration of recombinant CPs used in this experiment derived from clones pCymMV-M1 (M1-CP; Fig. 1), -M2 (M2-CP; Fig. 1) and -M2-CP-GL/AP (M2-CP-GL/AP; Fig. 6) and Glutathione-S-transferase (GST) derived from clones (pGEX 2T-1, Pharmacia Biosciences, Inc., New Jersey, USA) are shown. (C) Control experiments using M1 and M2 biotin-labeled RNA only (lane 1 and 2, respectively), or M1 and M2 RNA incubated with GST (lane 3 and 4, respectively) are shown. Because no RNA–protein binding occurred in these control experiments, RNA was detected only in S. (D) The results of experiments using RNA–protein combinations, M1 RNA/M1-CP (lane 1), M2 RNA/M1-CP (lane 2), M1 RNA/M2-CP (lane 3), M2 RNA/M2-CP (lane 4), M1 RNA/M2-CP-GL/AP (lane 5) and M2 RNA/M2-CP-GL/AP (lane 6), are shown. Different concentrations of sodium chloride (in milimolars; mM) added in incubation buffer are indicated. For convenience, the RNA–protein combinations used in the experiments are also indicated in the closed boxes. We repeated this experiment three times and one result is shown. The average S/P ratios were derived from the average of three independent experiments, and data were analyzed by Dunnett's *T* test. *indicates significant difference ($P<0.01$).

with substitution mutations within the transmembrane domain is restricted to a single cell, and PVX with mutations outside the transmembrane domain show reduced movement between cells and may not move systemically (Krishnamurthy et al., 2003). The amino acids identified in TGBp3 which are important for CymMV-M2 movement in *N. benthamiana* are not located in the *trans*membrane domain (Fig. 9; Krishnamurthy et al., 2003). Because all amino acids identified in CymMV TGBp1 and TGBp3 are not located in the conserved motifs previously identified among potexviruses, nor within the amino acids reported as essential for potexvirus movement, we speculate that changes in these regions may only slightly affect but not abolish the function (as we see in the case of CymMV-M2 CP) of TGBp1 and TGBp3, and the differential function required for virus movement is host dependent. This may explain why M1 and M2 can both systemically infect *Phalaenopsis* orchid, but only M1 can systemically infect *N. benthamiana*.

Table 1
Determination of interactions among CymMV encoded triple gene block proteins by yeast two-hybrid assay.

AD fusion[a]	BD fusion[a]	Trp− and Leu− medium[b]	Trp−, Leu−, His− and Ade− medium[c]	Histochemical assay[d] (X-α-gal)
T-antigen[e]	p53[e]	+++	+++	+++
TGBp1	*	+++	−	NA
TGBp2	*	+++	−	NA
TGBp3	*	+++	−	NA
CP	*	+++	−	NA
*	TGBp1	+++	−	NA
*	TGBp2	+++	−	NA
*	TGBp3	+++	−	NA
*	CP	+++	−	NA
TGBp1	TGBp1	+++	+++	+++
TGBp1	TGBp2	+++	−	NA
TGBp1	TGBp3	+++	−	NA
TGBp3	TGBp1	+++	−	NA
TGBp3	TGBp3	+++	−	NA
CP	CP	+++	+++	+++

[a] "*", plasmid expression AD domain (pGADT7) and BD domain (pGBKT7) are added.
[b] "+", yeast colonies that grew on SD medium (Lacking Trp and Leu). "−", yeast colonies that did not grow on SD medium (lacking Trp and Leu).
[c] "+", yeast colonies that grew on SD medium (Lacking Trp, Leu, His and Ade). "−", yeast colonies that did not grow on SD medium (Lacking Trp, Leu, His and Ade).
[d] "+", yeast colonies that were blue. "NA" indicates yeast colonies did not grow and no blue histochemical stain was observed.
[e] Plasmids containing T-antigen-AD and murine p53-BD were provided by the manufactory and used as positive controls.

It is worth noting that correct matching of the particular movement accessory components also includes the CymMV 5′ RNA sequence and/or the RNA-dependent RNA polymerase (RdRp). The potexvirus RdRp has not been reported to be required for virus movement, however it has been suggested that the 5′ untranslated region of the potexvirus genomic RNA plays a role in viral cell-to-cell movement (Lough et al., 2006).

Both CymMV-M1 and -M2 replicated well in *N. benthamiana* protoplasts or in *Phalaenopsis* orchids. It seems more likely that RNA rather than the RdRp plays a role in CymMV movement. However, recently it was reported that the TMV replicase and movement protein function together in altering plasmodesmeta (Guenoune-Gelbart et al., 2008). Therefore, we cannot rule out the possibility that the RdRp plays a role in controlling CymMV movement in *N. benthamiana* plants.

Materials and methods

RNA extraction and northern blot hybridization

RNA was extracted from plants as described for northern blot analysis and RT-PCR (Tian et al., 1996). T7 RNA polymerase and HpaI-digested pCymMV-M1 plasmids (CymMV probe; corresponding to the 590 nt of CymMV at its 3′ end) were used to generate the negative-sense DIG-labeled probes (Roche Applied Science; Mannheim, Germany). Northern blot hybridization was performed as described (Klaassen et al., 1996), and hybridization signals were detected by use of the chemiluminescent substrate CDP *STAR* (Roche Applied Science) and exposing blots to Fuji medical X-ray film (Fuji, Tokyo, Japan).

Construction of CymMV infectious clones and derived expression vectors

The construction of pCymMV-M1 and pCymMV-M1-green fluorescent protein (Fig. 1A) was as described (Lu et al., 2007). The same approaches were used to construct pCymMV-M2 and pCymMV-M2-GFP. Both pCymMV-M1 and -M2 had been completely sequenced. pCymMV-R- is a spontaneous mutation clone obtained during the cloning of pCymMV-M1. pCymMV-R- contains a mutation in the RNA-dependent RNA polymerase (RdRp) region, which causes pre-termination of the RdRp (Fig. 1A). The 5′ mutated RdRp region of the pCymMV-R- has been sequenced.

Construction of CymMV recombinant clones

The infectious clones pCymMV-M1 and pCymMV-M2 (Fig. 1A) were digested with NaeI and NheI individually. Two digested fragments derived from each reaction were gel purified by use of a gel extraction kit (Qiagen; Hilden, Germany); the small fragments derived from pCymMV-M1 and -M2 were exchanged and ligated by use of T4 DNA ligase (Promega; Madison, WI, USA) to construct pCymMV-M1/RdRp-M2 and pCymMV-M2/RdRp-M1 (Figs. 3C and D). The gel purification and ligation conditions followed the manufacturer's manual. The construction of pCymMV-M1/TGB-M2, pCymMV-M1/TGB-M1, pCymMV-M1/CP-M2 and pCymMV-M1/CP-M1 clones (Figs. 3E–H) was similar to that of pCymMV-M1/RdRp-M2 and pCymMV-M2/RdRp-M1, except the restriction enzymes NheI and HpaI were used to construct pCymMV-M1/TGB-M2 and pCymMV-M2/TGB-M1, and the restriction enzymes HpaI and SacI was used to construct pCymMV-M1/CP-M2 and pCymMV-M2/CP-M1. All recombinant clones were sequenced in the modified region to ensure that the clones were correct.

Construction of TGBps recombinant clones

pCymMV-M1 and pCymMV-M2 were used as the initial template, and the primer pairs CymMV F3783/CymMV-TGB1 R and CymMV-TGB1 F/CymMV CPR (Supplementary Table S1) were used, respectively in the PCR reactions to amplify the two overlapping fragments. The amplified fragments were gel purified and mixed together at a ratio of 1:1, then used in another PCR reaction. The PCR reaction cycles were 94 °C for 5 min for 1 cycle, then 94 °C for 30 s, 55 °C for 30 s and 72 °C for 2 min for a total of 5 cycles. Then the primer pair CymMV F3783/CymMV CPR was added for another 30 cycles. The PCR cycles were 94 °C for 5 min for 1 cycle, then 94 °C for 30 s, 55 °C for 30 s and 72 °C for 2 min for a total of 30 cycles. The amplified products were digested with NheI and HpaI (Fig. 3), and then separated on a 1% agarose gel to purify the 1.3-kb fragment. The pCymMV-M2 was digested with NheI and HpaI, then separated on 1% agarose gel to purify the 8-kb fragment. Both digested fragments were ligated to yield a construct pCymMV-M2/TGB1-M1 (Fig. 4C). The construction of other recombinant TGB clones (Figs. 4D–H) was essentially the same as that for pCymMV-M2/TGB1-M1, except that different primer pairs and templates were used. The primer CymMV F3783/TGB1 and CymMV CPR were used in construction of all TGB recombinant clones. The clone name indicates the origin of the TGB. For example, pCymMV-M2/TGB1-M1 indicates that the backbone of the clone is pCymMV-M2, but the TGBp1 is derived from pCymMV-M1. For construction of pCymMV-M2/TGB2-M1, an intermediate clone, pCymMV-M1/TGB1-M2 was first constructed and used for a template to amplify the M2 TGBp1 and M1 TGBp2. The amino acid sequences in an overlapping region between TGBp1 and TGBp2 and between TGBp2 and TGBp3 are identical in both pCymMV-M1 and -M2. All primers are shown in Supplementary Table S1. All recombinant clones were sequenced in the modified region to ensure that the clones were correct.

Site-directed mutagenesis

Each of the mutated clones derived from pCymMV-M1/M2 with amino acid substitution(s) in the CP, TGBp1 and TGBp3 (Figs. 6, 8) was constructed by site-directed mutagenesis as described (Lu et al., 2007). pCymMV-M1 was used as the initial template, and the primer pairs CymMV F3783/TGB1 Y44H R and TGB1 Y44H F/CymMV CPR were used in the first PCR reactions. The amplified fragments were gel purified and mixed together at a ratio of 1:1, then used in another PCR reaction. The PCR reaction cycles were as described above. The amplified products were digested with NheI and HpaI (Fig. 3), and then separated on a 1% agarose gel to purify the 1.3-kb fragment. The pCymMV-M2 was digested with NheI and HpaI, then separated on a 1% agarose gel to purify the 8-kb fragment. Both digested fragments were ligated to construct

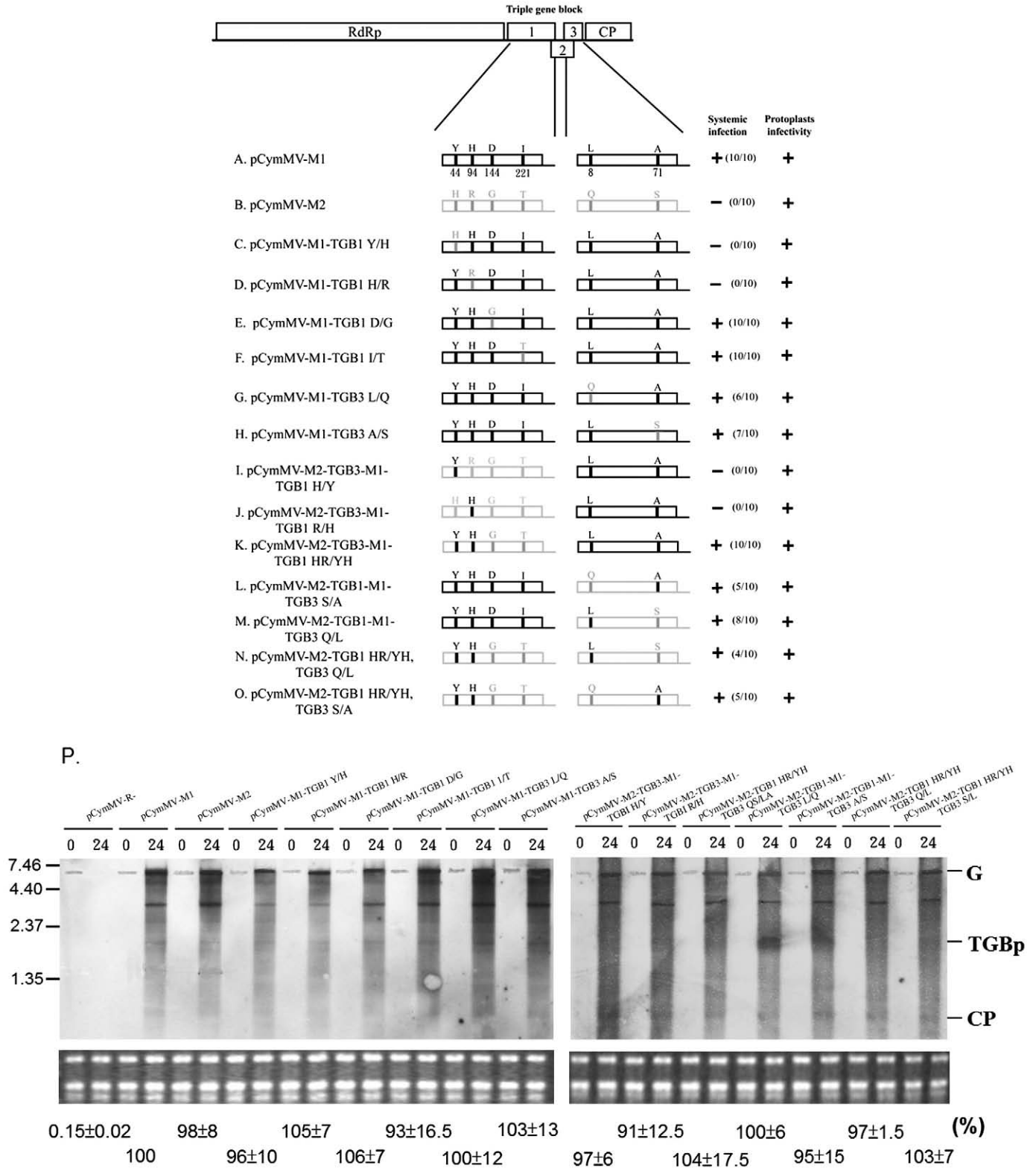

Fig. 8. Schematic representation of TGBp1 mutants and infectivity assay between pCymMV-M1 and pCymMV-M2. (A–O) Rectangles represent ORFs encoded by CymMV genomic RNA, RNA-dependent RNA polymerase (RdRp), triple gene block ORFs 1, 2, and 3 and capsid protein (CP). Black and gray lines indicate different amino acids between pCymMV-M1 and pCymMV-M2, respectively. Positions of amino acids are indicated. Chimeric viruses competent in protoplast accumulation and systemic infection in *N. benthamiana* plants are indicated by +, and the ratio of systemic infected to total inoculated plants is indicated. Systemic infection was detected 2 weeks post-inoculation by RT-PCR. (P) Protoplast infectivity was detected 24 h post-inoculation by northern blot hybridization, and the ribosomal RNA used for a loading control are indicated. Genomic RNA (G), TGBp, and CP subgenomic RNA are indicated. The pCymMV-R- used as a negative control is illustrated in Fig. 1. The average percentage of relative real-time RT-PCR quantification (from 3 independent experiments) of CymMV RNA from CymMV clone-infected protoplasts at 24 h post-inoculation is indicated below the gels. The accumulation of pCymMV-M1 was set at 100% for relative quantification. Numbers at the left correspond to positions of marker RNAs (sizes in 1000 nucleotides) analyzed in the same gel.

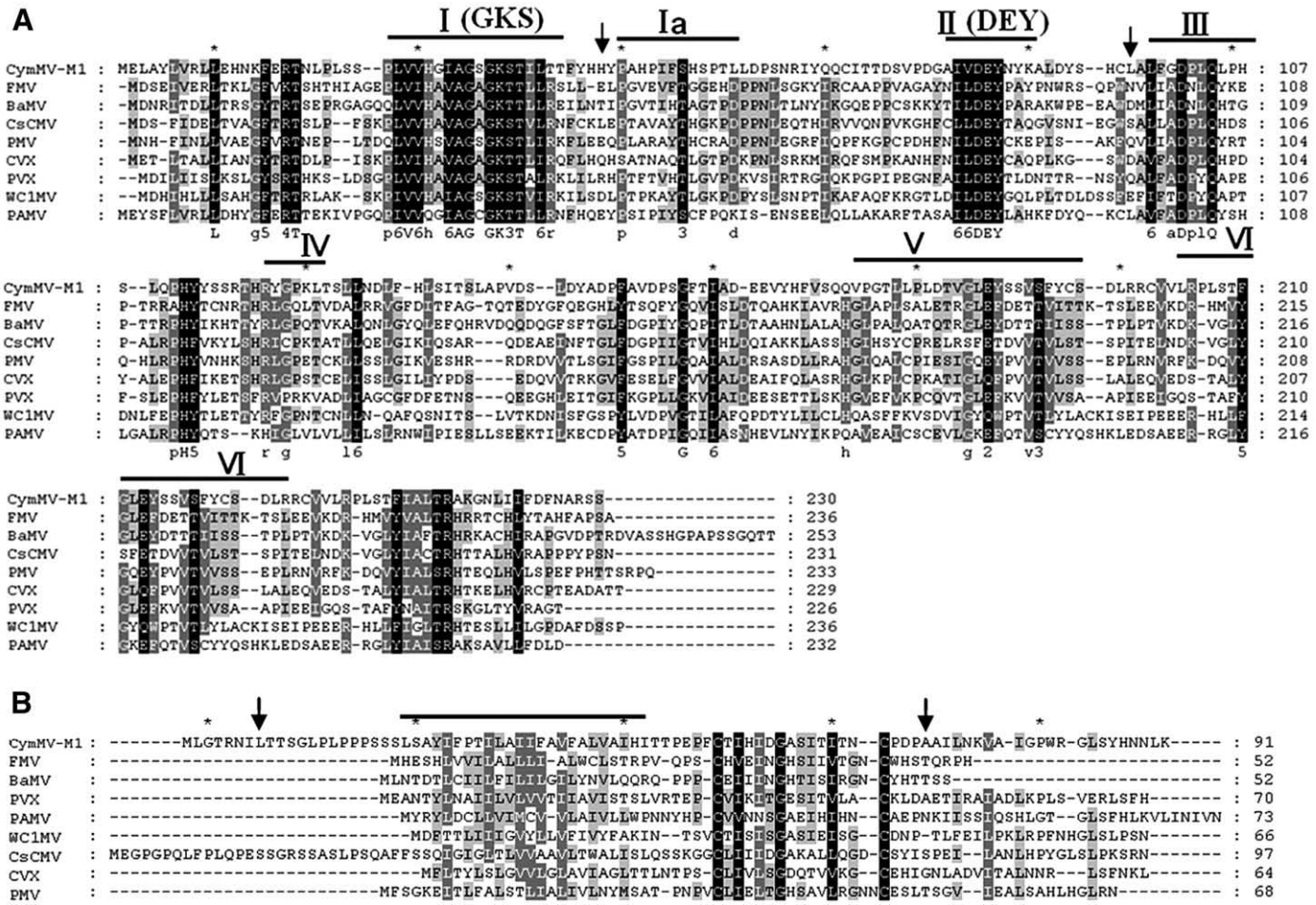

Fig. 9. The amino acid sequence alignment of TGBp1 NTP/helicase domain and TGBp3 transmembrane domain of potexvirus. The amino acid sequence alignments were conducted by use of clustal X 1.83 (Thompson et al., 1997). (A) The conserved motifs of the potexvirus NTPase/helicase domain were previously predicted (Kalinina et al., 2002). The 7 predicted NTPase/helicase motifs of potexvirus TGBp1 are shown, and two canonical motifs of NTPase, DEY and GKS, are indicated. The arrows indicate the amino acid positions important for pCymMV-M2 to systemically infect *N. benthamiana*. (B) The potexvirus TGBp3 transmembrane domain was previously identified (Krishnamurthy et al., 2003). The CymMV transmembrane domain predicted by DAS program (http://www.sbc.su.se/~miklos/DAS/maindas.html) is indicated by a thick black line. The arrows indicate the amino acids important for pCymMV-M2 to systemically infect *N. benthamiana*. The viruses, abbreviation and accession number used in alignments of TGBp1 NTP/helicase and TGbp3 transmembrane domains are described below. *Cymbidium mosaic virus* (CymMV, accession number AY571289); *Cymbidium mosaic virus* (CymMV, accession number AY571289); *Foxtail mosaic virus* (FMV, accession number NC_001483); *Watermelon spotted wilt virus* (BSMV, accession number NC_003481); *Cassava common mosaic virus* (CsCMV, accession number NC_001658); *Papaya mosaic virus* (PMV, accession number NC_001748); *Cactus virus X* (CVX, accession number NC_002815); *Potato virus X* (PVX, accession number NC_001455); *White clover mosaic virus* (WC1MV, accession number X06728).

pCymMV-M1-TGB1 Y/H containing a single substitution (Y/H) at amino acid position 44 of TGBp1 of pCymMV-M1 (Fig. 8C). The construction of other TGB site-directed mutagenesis clones (Fig. 8) was essentially the same as that for pCymMV-M1-TGB1 Y/H, except that different primer pairs and templates were used. The primer CymMV F3783/TGB1 and CymMV CPR were used in construction of all mutant clones. The remaining primers are in Supplementary Table S1. The mutated clones with names beginning with pCymMV-M1- or -M2- indicate that the initial template was pCymMV-M1 or pCymMV-M2, respectively. Modifications of nucleotide sequence in an overlapping region between TGBp1 and TGBp2 (one nucleotide substitution) and between TGBp2 and TGBp3 (two nucleotides substitution) do not cause amino acid sequence changes in TGBp2. All mutant clones were sequenced in the modified region to ensure that the mutations were correct.

Preparation and transfection of N. benthamiana protoplasts

Capped transcripts corresponding to the wild-type virus and the constructed vectors of CymMV were synthesized by use of the mMESSAGE mMACHINE T3 high yield capped RNA transcription kit (Ambion, Inc., Austin, TX). In total, 5 μg of pCymMV-M1 and its derivative plasmids were digested with SpeI and in vitro transcription was conducted according to manufacturer's instruction. Protoplasts prepared from *Nicotiana benthamiana* plants and RNA transfection were as previously described (Satyanarayana et al., 2002), except that 10 μg of each transcript and 2×10^5 cells were used for each inoculation, and after inoculation, protoplasts were incubated at 26 °C. The inoculated protoplasts were collected as previously described (Klaassen et al., 1996). Aliquots containing approximately 1×10^5 cells were collected by centrifugation (1300 ×*g*) at different times post-inoculation, and RNA was isolated by use of TRIzol Reagent (Invitrogen, San Diego, CA) according to the manufacturer's recommendations. The RNA was dissolved in 30 μl DEPC-treated water, and 5 μg RNA (equivalent to 5×10^4 cells) was used for northern hybridization analysis.

Plants and virus inoculation

An amount of 5 μg transcripts was dissolved in inoculation buffer (0.05 M NaH_2PO_4/Na_2HPO_4 pH 7.0) and rubbed to carborundum-dusted *Phalaenopsis* var. *formosa* (6 leaf stage) or *N. benthamiana* (5 leaf stage) by hands wearing latex gloves. The inoculated leaves were washed with excess distilled water, and the viruses were detected 2 weeks post-inoculation. All plants were kept in an insect-proof and

thermal-controlled (25 °C–28 °C) greenhouse and with 12 h of light (5.22 μmol/$s^{-1}m^{-2}$) for two weeks. *P. amabilis* var. *formosa* (10 cm in height) was purchased from the Taiwan Sugar Research Institute (Tainan, Taiwan). Each set of inoculations (Figs. 3, 4, 6 and 8) was repeated at least three times. RT-PCR was used to amplify the modified region (primer pairs used for RT-PCR were described in Supplementary Table 1) of each mutated CymMV from two randomly selected plants of each inoculation set followed by sequencing, all detected progeny viruses still maintained the original modification.

RT-PCR

RNA extracted from CymMV-infected plants was used as a template for synthesis of cDNAs by Moloney murine leukaemia virus (MMLV) reverse transcriptase following the manufacturer's instructions (Promega, Inc., Madison, WI, USA). The PCR amplification conditions were as described (Rubio et al., 2000). The cDNAs were PCR amplified in a mixture containing 1.5 mM $MgCl_2$, 1 mM of each of the 4 dNTPs, 2.5 U of Taq DNA polymerase (Promega, Inc., Madison, USA), and 50 ng of each oligonucleotide. The PCR cycles were 94 °C for 4 min for 1 cycle, then 94 °C for 30 s, 55 °C for 30 s and 72 °C for 1 min for 30 cycles, then an extension at 72 °C for 10 min.

Construction of CymMV CP expression clones

pCymMV-M1 and pCymMV-M2 were used as the initial template, and the primer pairs CymMV CP-BamHI F and CymMV CP-BamHI R (Supplementary Table S1) were used in the PCR reactions to amplify the two CymMV CP fragments. The fragments were gel purified by use of a gel extraction kit (Qiagen) and digested with BamHI. The fragment derived from pCymMV-M1 and pCymMV-M2 was incubated with the BamHI-digested expression vector pGEX-2T and ligated by use of T4 DNA ligase (Promega) to construct pGEX-2T-2:M1CP and pGEX-2T-2:M2CP. Both clones had been sequenced completely.

Expression and purification of CymMV CP

A total of 5 ml of overnight cultures of *Escherichia coli* XL1-blue transformed with pGEX-2T-2:M1CP, pGEX-2T-2:M2CP and pGEX-2T, were diluted 1:100 with 50 ml Luria–Bertani medium (LB) containing ampicillin (50 μg/ml), and grown until they reached the OD_{600} = 1.0 at 37 °C. 200 ml LB medium containing ampicillin (50 μg/ml) was added, and bacteria were grown until they reached the OD_{600} = 0.5 at 37 °C. Then the fusion protein expression was induced with 1 mM isopropyl-β-D-thiogalactopyranoside (IPTG) for 2 h at 37 °C. After centrifugation at 5000 ×*g* for 10 min at 4 °C, the pellet was suspended in a 10 ml phosphate buffer saline (PBS) (135 mM NaCl, 2.7 mM KCl, 1.5 mM KH_2PO_4, and 8 mM K_2HPO_4, pH 7.2) and incubated in 1% Triton X-100 for 60 min at 4 °C then disrupted by sonication. Cell debris was removed by centrifugation for 5 min at 4 °C at 13,000 ×*g*. Glutathione Sepharose beads were added and incubated for 4 h at 4 °C. After centrifugation at 3000 ×*g* for 5 min at 4 °C, the pellet was suspended in 1 ml PBS and the wash was repeated 4 times. Finally, 500 μl Elution buffer (10 mM reduced glutathione; 50 mM Tris–HCl pH 8.0) was added, samples were centrifuged at 500 ×*g* for 5 min at 4 °C, the suspension was collected and analyzed in 12% SDS-PAGE gels (Laemmli, 1970).

Protein–RNA pull-down assay

The pCymMV-M1 and pCymMV-M2 RNA transcripts were synthesized by use of the mMESSAGE mMACHINE T3 high yield capped RNA transcription kit (Ambion). The biotinylated diribonucleotide, pUC-biotin (Midland Certified Reagents, Inc. Midland, Texas, USA) was ligated to transcripts with T4 RNA ligase. The biotin-labeled CymMV RNA was incubated with glutathione-S-transferase (GST) fused to CymMV CP in 100 μl incubation buffer (10 mM Tris/HCl and 150 mM NaCl, 1 mM EDTA, 5 mM $MgCl_2$, 1 mM dithiothreitol, pH 7.6) at 20 °C for 2 h. Glutathione Sepharose beads were added and incubated at 4 °C for 4 h. After centrifugation at 3000 ×*g* for 5 min at 4 °C, the supernatant was removed and the pellet was re-suspended in incubation buffer of different concentrations (150, 300, 400 and 1000 mM) of sodium chloride. After centrifugation at 3000 ×*g* at 4 °C for 5 min, supernatant (defined here as S) and pellets were collected. The pellets were re-suspended in high salt incubation buffer (1 M of sodium chloride) to separate the CymMV CP–RNA complex from Glutathione Sepharose beads. After centrifugation at 3000 ×*g* at 4 °C for 5 min, the supernatant (defined here as P) were collected. The collected S and P were passed through Hybond-NX membrane (Amersham GE Healthcare, Inc., Piscataway, NJ, USA) using a slot-blot apparatus (Schleicher and Schuell, Inc., Keene, NH, USA). The membranes were baked at 80 °C for 30 min. The signals were detected first using antibody against biotin and by use of a LightShift Chemiluminescent EMSA kit (Pierce, Inc., Rockford, IL) followed the manufacturer's protocol for chemical illumination. Fluorescence signals were captured by use of a Biospectrum AC Imaging system (UVP, LLC., Upland, CA, USA).

Whole-mount RNA analysis

Whole-mount RNA analysis was as described with modification (Zachgo et al., 2000). Sample fixing was extended to 2 h RT in a glass vial in PBS containing 0.1% Tween 20, 0.08 M EGTA, 10% DMSO and 5% paraformaldehyde. CymMV CP probe (see above) was used for hybridization.

Construction of CymMV TGBp and CP yeast two-hybrid clones

pCymMV-M1 was used as the initial template, and the primer pairs TGB1F/TGB1R, TGB2F/TGB2R, TGB3F/TGB 3R, CPF/CPR (Supplementary Table S1) were used in PCR reactions to amplify the TGBp1, TGBp2, TGBp3 and CP fragments. The fragments were gel purified, incubated with the SmaI digested pGDAT7 and pGBKT7 (Clontech, Mountain View, CA), and ligated by use of T4 DNA ligase (Promega) to construct pTGB1-AD, pTGB2-AD, pTGB3-AD, pCP-AD, pTGB1-BD, pTGB2-BD, pTGB3-BD and pCP-BD. All clones had been sequenced completely.

Yeast two-hybrid system

Yeast two-hybrid assays were done by use of the Matchmaker Yeast Two-Hybrid System 3 (Clontech) following the manufacturer's instructions. Yeast was transformed with bait vectors and prey vectors and selected on SD plates lacking Leu and Trp. After 2 days of growth at 30 °C, the yeast colonies were transferred to two different selection plates containing SD medium lacking Leu, Trp, and SD medium (containing X-α-GAL) lacking Leu, Trp and His.

Statistical analysis

Statistical analysis involved ANOVA or Dunnett's *T* test with use of MINITAB14 (Minitab Inc., State College, PA, USA).

Appendix A. Supplementary data

Supplementary data associated with this article can be found, in the online version, at doi:10.1016/j.virol.2009.02.049.

References

Abouhaidar, M.G., Lai, R., 1989. Nucleotide sequence of the 3′-terminal region of clover yellow mosaic virus RNA. J. Gen. Virol. 70, 1871–1875.

Adams, M.J., Accotto, G.P., Agranovsky, A.A., Bar-Joseph, M., Boscia, D., Brunt, A.A., Candresse, T., Coutts, R.H.A., Dolja, V.V., Falk, B.W., Foster, G.D., Gonsalves, D., Jelkmann, W., Karasev, A., Martelli, G.P., Mawassi, M., Milne, R.G., Minafra, A., Namba, S., Rowhani, A., Vetten, H.J., Vishnichenko, V.K., Wisler, G.C., Yoshikawa, N., Zavriev, S.K., 2005a. Genus Potexvirus. In: Fauquet, C.M., Mayo, M.A., Maniloff, J.,

Desselberger, U., Ball, L.A. (Eds.), Virus Taxonomy: Eighth Report of the International Committee on Taxonomy of Virus. Elsevier Academic Press, San Diego, CA, pp. 1091–1095.
Adams, M.J., Accotto, G.P., Agranovsky, A.A., Bar-Joseph, M., Boscia, D., Brunt, A.A., Candresse, T., Coutts, R.H.A., Dolja, V.V., Falk, B.W., Foster, G.D., Gonsalves, D., Jelkmann, W., Karasev, A., Martelli, G.P., Mawassi, M., Milne, R.G., Minafra, A., Namba, S., Rowhani, A., Vetten, H.J., Vishnichenko, V.K., Wisler, G.C., Yoshikawa, N., Zavriev, S.K., 2005b. *Flexiviridae*. In: Fauquet, C.M., Mayo, M.A., Maniloff, J., Desselberger, U., Ball, L.A. (Eds.), Fauquet, Virus Taxonomy : Eight Report of the International Committee on Taxonomy of Viruses. Elsevier Academic Press, San Diego, CA, pp. 1101–1124.
Angell, S.M., Davies, C., Baulcombe, D.C., 1996. Cell-to-cell movement of potato virus X is associated with a change in the size-exclusion limit of plasmodesmata in trichome cells of *Nicotiana clevelandii*. Virology 216, 197–201.
Bayne, E.H., Rakitina, D.V., Morozov, S.Y.u., Baulcombe, D.C., 2005. Cell-to-cell movement of potato potexvirus X is dependent on suppression of RNA silencing. Plant J. 44, 471–482.
Beck, D.L., Guilford, P.J., Voot, D.M., Andersen, M.T., Forster, R.L., 1991. Triple gene block proteins of white clover mosaic potexvirus are required for transport. Virology 183, 695–702.
Chapman, S., Hills, G., Watts, J., Baulcombe, D.C., 1992. Mutational analysis of the coat protein gene of potato virus X: effects on virion morphology and viral pathogenicity. Virology 191, 223–230.
Cheo, P.C., 1970. Subliminal infection of cotton by Tobacco Mosaic Virus. Phytopathology 60, 41–46.
Cruz, S.S., Roberts, A.G., Prior, D.A., Chapman, S., Oparka, K.J., 1998. Cell-to-cell and phloem-mediated transport of potato virus X. The role of virions. Plant Cell 10, 495–510.
Fedorkin, O., Solovyev, A., Yelina, N., Zamyatnin, A.J.R., Zinovkin, R., Makinen, K., Schiemann, J., Morozov, S.Y.u., 2001. Cell-to-cell movement of potato virus X involves distinct functions of the coat protein. J. Gen. Virol. 82, 449–458.
Forster, R.L., Beck, D.L., Guilford, P.J., Voot, D.M., Van Dolleweerd, C.J., Andersen, M.T., 1992. The coat protein of white clover mosaic potexvirus has a role in facilitating cell-to-cell transport in plants. Virology 191, 480–484.
Fujita, Y., Mise, K., Okuno, T., Ahlquist, P., Furusawa, I., 1996. A single codon change in a conserved motif of a bromovirus movement protein gene confers compatibility with a new host. Virology 223, 283–291.
Guenoune-Gelbart, D., Elbaum, M., Sagi, G., Levy, A., Epel, B.L., 2008. Tobacco mosaic virus (TMV) replicase and movement protein function synergistically in facilitating TMV spread by lateral diffusion in the plasmodesmal desmotubule of *Nicotiana benthamiana*. Mol. Plant-Microb. Interact. 21, 335–345.
Harrison, H.L., 1969. Optimize switching circuits using Karnaugh maps. Control Eng. 16, 87–88.
Howard, A.R., Heppler, M.L., Ju, H.J., Krishnamurthy, K., Payton, M.E., Verchot-Lubicz, J., 2004. Potato virus X TGBp1 induces plasmodesmata gating and moves between cells in several host species whereas CP moves only in *N. benthamiana* leaves. Virology 328, 185–197.
Ju, H.J., Brown, J.E., Ye, C.M., Verchot-Lubicz, J., 2007. Mutations in the central domain of potato virus X TGBp2 eliminate granular vesicles and virus cell-to-cell trafficking. J. Virol. 81, 1899–1911.
Kadare, G., Haenni, A.L., 1997. Virus-encoded RNA helicases. J. Virol. 71, 2583–2590.
Kalinina, N.O., Rakitina, D.V., Solovyev, A.G., Schiemann, J., Morozov, S.Y.u., 2002. RNA helicase activity of the plant virus movement proteins encoded by the first gene of the triple gene block. Virology 296, 321–329.
Karpova, O.V., Zayakina, O.V., Arkhipenko, M.V., Sheval, E.V., Kiselyova, O.I., Poljakov, V.Y., Yaminsky, I.V., Rodionova, N.P., Atabekov, J.G., 2006. Potato virus X RNA-mediated assembly of single-tailed ternary 'coat protein-RNA-movement protein' complexes. J. Gen. Virol. 87, 2731–2740.
Klaassen, V.A., Mayhew, D., Fisher, D., Falk, B.W., 1996. In vitro transcripts from cloned cDNAs of the lettuce infectious yellows closterovirus bipartite genomic RNAs are competent for replication in *Nicotiana benthamiana* protoplasts. Virology 222, 169–175.
Krishnamurthy, K., Mitra, R., Payton, M.E., Verchot-Lubicz, J., 2002. Cell-to-cell movement of the PVX 12K, 8K, or coat proteins may depend on the host, leaf developmental stage, and the PVX 25K protein. Virology 300, 269–281.
Krishnamurthy, K., Heppler, M., Mitra, R., Blancaflor, E., Payton, M., Nelson, R.S., Verchot-Lubicz, J., 2003. The potato virus X TGBp3 protein associates with the ER network for virus cell-to-cell movement. Virology 309, 135–151.
Laemmli, U.K., 1970. Cleavage of structural proteins during the assembly of the head of bacteriophage T4. Nature 227, 680–685.
Leshchiner, A.D., Solovyev, A.G., Morozov, S.Y.u., Kalinina, N.O., 2006. A minimal region in the NTPase/helicase domain of the TGBp1 plant virus movement protein is responsible for ATPase activity and cooperative RNA binding. J. Gen. Virol. 87, 3087–3095.
Lin, M.K., Chang, B.Y., Liao, J.T., Lin, N.S., Hsu, Y.H., 2004. Arg-16 and Arg-21 in the N-terminal region of the triple-gene-block protein 1 of Bamboo mosaic virus are essential for virus movement. J. Gen. Virol. 85, 251–259.
Lin, M.K., Hu, C.C., Lin, N.S., Chang, B.Y., Hsu, Y.H., 2006. Movement of potexviruses requires species-specific interactions among the cognate triple gene block proteins, as revealed by a trans-complementation assay based on the bamboo mosaic virus satellite RNA-mediated expression system. J. Gen. Virol. 87, 1357–1367.
Lough, T.J., Shash, K., Xoconostle-Cazeres, B., Hofstra, K.R., Beck, D.L., Balmori, E., Forster, R.L., Lucas, W.J., 1998. Molecular dissection of the mechanism by which potexvirus triple gene block proteins mediate cell-to-cell transport of infectious RNA. Mol. Plant-Microb. Interact. 11, 801–814.
Lough, T.J., Netzler, N.E., Emerson, S.J., Sutherland, P., Carr, F., Beck, D.L., Lucas, W.J., Forster, R.L., 2000. Cell-to-cell movement of potexviruses: evidence for a ribonucleoprotein complex involving the coat protein and first triple gene block protein. Mol. Plant-Microb. Interact. 13, 962–974.
Lough, T.J., Emerson, S.J., Lucas, W.J., Forster, R.L., 2001. Trans-complementation of long-distance movement of white clover mosaic virus triple gene block (TGB) mutants: phloem-associated movement of TGBp1. Virology 288, 18–28.
Lough, T.J., Lee, R.H., Emerson, S.J., Forster, R.L., Lucas, W.J., 2006. Functional analysis of the 5′ untranslated region of potexvirus RNA reveals a role in viral replication and cell-to-cell movement. Virology 351, 455–465.
Lu, H.C., Chen, H.H., Tsai, W.C., Chen, W.H., Su, H.J., Chang, D.C., Yeh, H.H., 2007. Strategies for functional validation of genes involved in reproductive stages of orchids. Plant Physiol. 143, 558–569.
Lucas, W.J., 2006. Plant viral movement proteins: agents for cell-to-cell trafficking of viral genomes. Virology 344, 169–184.
Mitra, R., Krishnamurthy, K., Blancaflor, E., Payton, M., Nelson, R.S., Verchot-Lubicz, J., 2003. The potato virus X TGBp2 protein association with the endoplasmic reticulum plays a role in but is not sufficient for viral cell-to-cell movement. Virology 312, 35–48.
Morozov, S. Yu, Solovyev, A.G., 2003. Triple gene block: modular design of a multifunctional machine for plant virus movement. J. Gen. Virol. 84, 1351–1366.
Morozov, S. Yu, Fedorkin, O.N., Juttner, G., Schiemann, J., Baulcombe, D.C., Atabekov, J.G., 1997. Complementation of a potato virus X mutant mediated by bombardment of plant tissues with cloned viral movement protein genes. J. Gen. Virol. 78, 2077–2083.
Morozov, S. Yu, Solovyev, A.G., Kalinina, N.O., Fedorkin, O.N., Samuilova, O.V., Schiemann, J., Atabekov, J.G., 1999. Evidence for two nonoverlapping functional domains in the potato virus X 25K movement protein. Virology 260, 55–63.
Rubio, L., Yeh, H.H., Tian, T., Falk, B.W., 2000. A heterogeneous population of defective RNAs is associated with lettuce infectious yellows virus. Virology 271, 205–212.
Saenz, P., Salvador, B., Simon-Mateo, C., Kasschau, K.D., Carrington, J.C., Garcia, J.A., 2002. Host-specific involvement of the HC protein in the long-distance movement of potyviruses. J. Virol. 76, 1922–1931.
Samuels, T.D., Ju, H.J., Ye, C.M., Motes, C.M., Blancaflor, E.B., Verchot-Lubicz, J., 2007. Subcellular targeting and interactions among the potato virus X TGB proteins. Virology 367, 375–389.
Satyanarayana, T., Gowda, S., Ayllon, M.A., Albiach-Marti, M.R., Rabindran, S., Dawson, W.O., 2002. The p23 protein of citrus tristeza virus controls asymmetrical RNA accumulation. J. Virol. 76, 473–483.
Sulzinski, M.A., Zaitlin, M., 1982. Tobacco mosaic virus replication in resistant and susceptible plants: in some resistant species virus is confined to a small number of initially infected cells. Virology 121, 12–19.
Tamai, A., Meshi, T., 2001. Cell-to-cell movement of potato virus X: the role of p12 and p8 encoded by the second and third open reading frames of the triple gene block. Mol. Plant Microbe. Interact. 14, 1158–1167.
Thompson, J.D., Gibson, T.J., Plewniak, F., Jeanmougin, F., Higgins, D.G., 1997. The CLUSTAL_X windows interface: flexible strategies for multiple sequence alignment aided by quality analysis tools. Nucleic Acids Res. 25, 4876–4882.
Tian, T., Klaassen, V.A., Soong, J., Wisler, G., Duffus, J.E., Falk, B.W., 1996. Generation of cDNAs specific to lettuce infectious yellows closterovirus and other whitefly-transmitted viruses by RT-PCR and degenerate oligonucleotide primers corresponding to the closterovirus gene encoding the heat shock protein 70 homolog. Mol. Plant Pathol. 86, 1167–1173.
Timian, R.G., 1974. The range of symbiosis of barley and barley stripe mosaic virus. Phytopathology 64, 342–345.
Verchot-Lubicz, J., 2005. A new cell-to-cell transport model for potexviruses. Mol. Plant-Microb. Interact. 18, 283–290.
Verchot-Lubicz, J., Ye, C.M., Bamunusinghe, D.C., 2007. Molecular biology of potexviruses: recent advances. J. Gen. Virol. 88, 1643–1655.
Wang, H.L., Wang, Y., Giesman-Cookmeyer, D., Lommel, S.A., Lucas, W.J., 1998. Mutations in viral movement protein alter systemic infection and identify an intercellular barrier to entry into the phloem long-distance transport system. Virology 245, 75–89.
Yang, Y., Ding, B., Baulcombe, D.C., Verchot, J., 2000. Cell-to-cell movement of the 25K protein of potato virus X Is regulated by three other viral proteins. Mol. Plant-Microb. Interact. 13, 599–605.
Zachgo, S., Perbal, M.C., Saedler, H., Schwarz-Sommer, Z., 2000. In situ analysis of RNA and protein expression in whole mounts facilitates detection of floral gene expression dynamics. Plant J. 23, 697–702.
Zettler, F.W., Ko, N.J., Wisler, G.C., Elliott, M.S., Wong, S.M., 1990. Viruses of Orchids and their control. Plant Dis. 74, 621–626.